"Pulsating stars in the Milky Way"

Classical and Type-II Cepheids

Martin Groenewegen

Royal Observatory of Belgium, Brussels

(martin.groenewegen@oma.be)

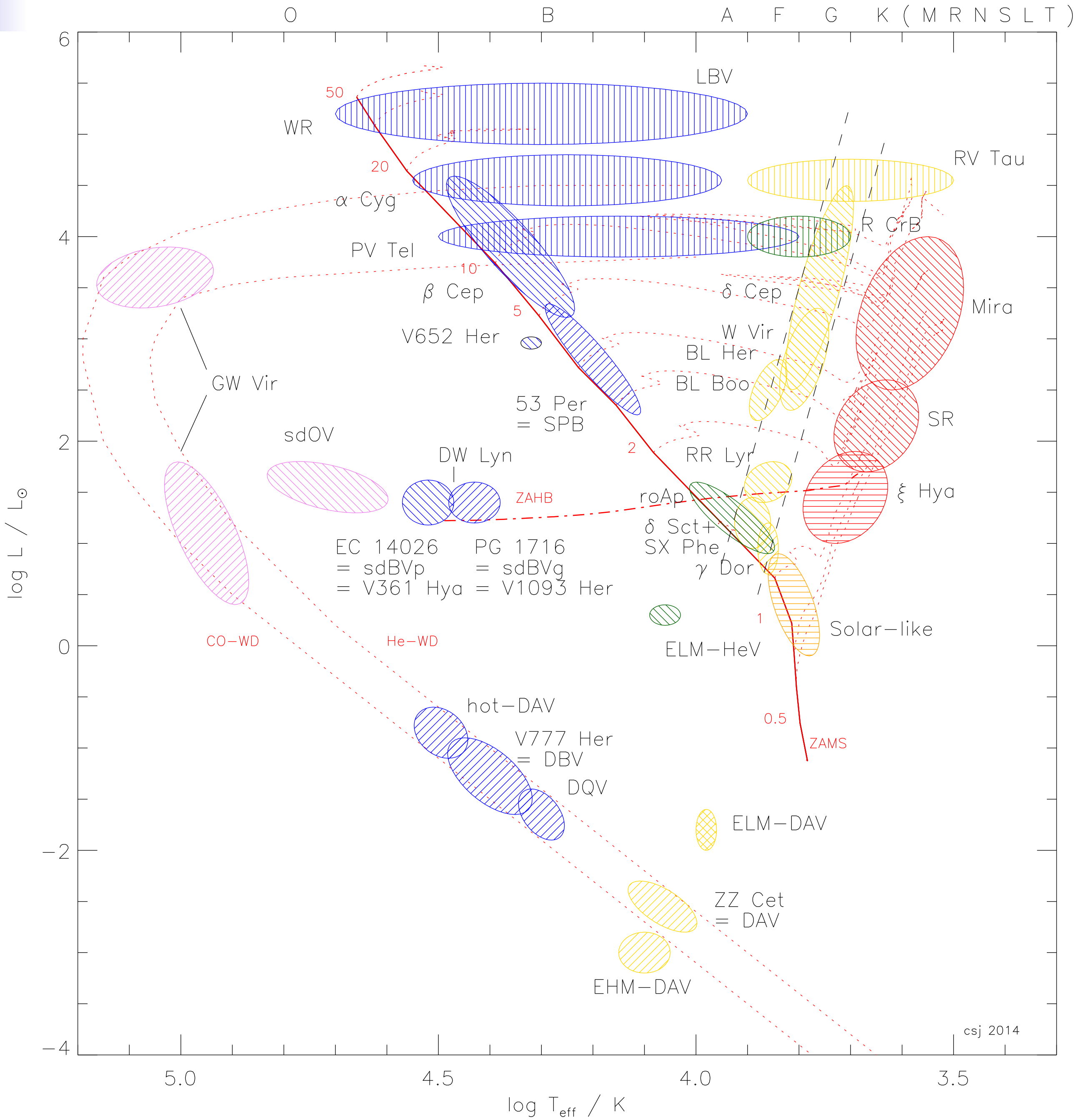

(from Jeffery, Saio, 2016, MNRAS, 458)

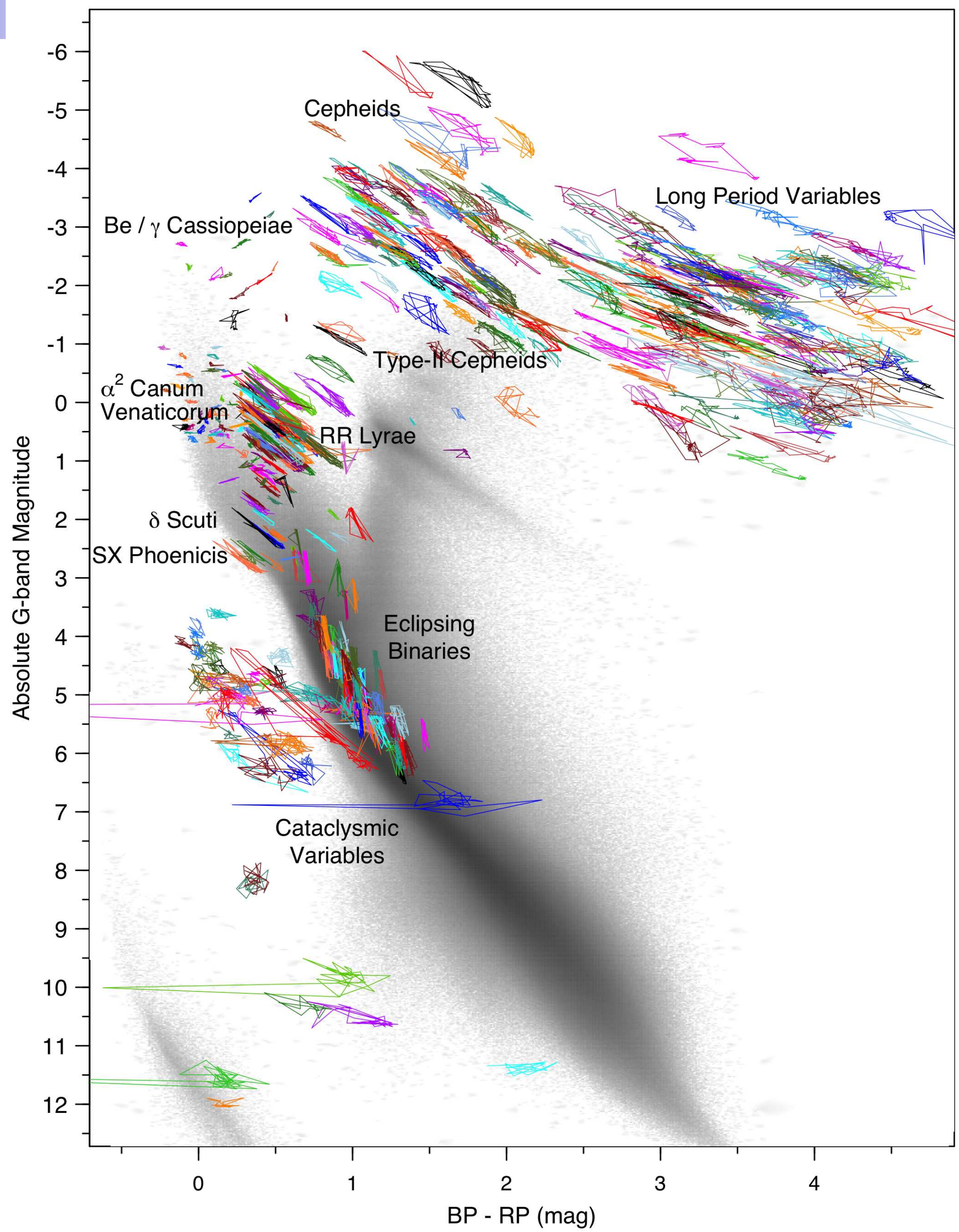

Gaia Collaboration, Eyer et al. arXiv:1804.09382 GDR2: Variable stars in the colour-absolute magnitude diagram

Overview Talk

- Type-II Cepheids
  (work with Monika Jurkovic, AOB,
  2017 A&A 603, A70 and A&A 604, A29)
- Classical Cepheids
  MW Cepheids with *Gaia*,
  classical PLZ-relations, DM to LMC
  (submitted)

T2C: What are they ?

- Gingold (1976, 1985), Wallerstein (2002), Sandage & Tammann (2006)
- BL Her (1-4d), evolving of HB towards the AGB
- W Vir (4-20d), blue-loop off the AGB after a TP
- RV Tau (20-70d), Post-AGB, evolving off the AGB

Binarity ?

- MCs: peculiar W Vir (pWVir)
- MCs: T2C in EBs
- Known Galactic RV Tau that have discs and are known binaries

OGLE sample in the MCs

	LMC	SMC
BL Her	64	17
W Vir	97	17
RV Tau	42	9
AC (F)	62	3
AC (1O)	21	3
		335

OGLE-III: Soszyński et al. (2008, 2010a, 2010b)

SED fitting

Construction of SED by collecting all available photometry
Fitting model atmosphere (+ dust shell)
For assumed distance (50, 61 kpc), get L, $T_{\rm eff}$, optical depth

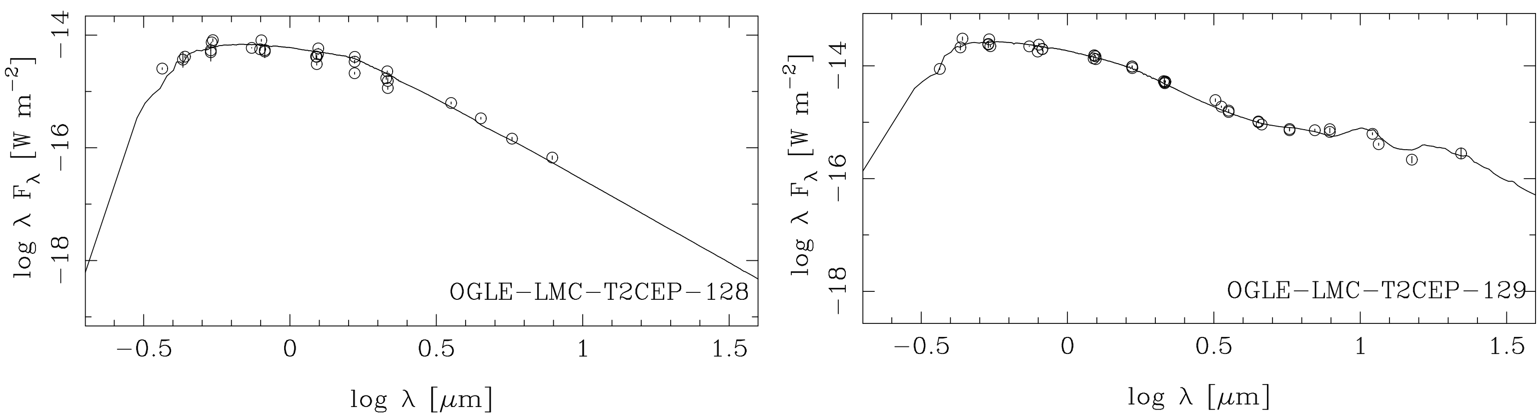

30 of 51 RVT have IR emission (27/42 LMC; 3/9 SMC)
Surprise: 11 of 114 W Vir have excess emission (8/97 LMC; 3/17 SMC; 3/24 pWVir)
0/81 BLH, 0/88 AC

IR excess

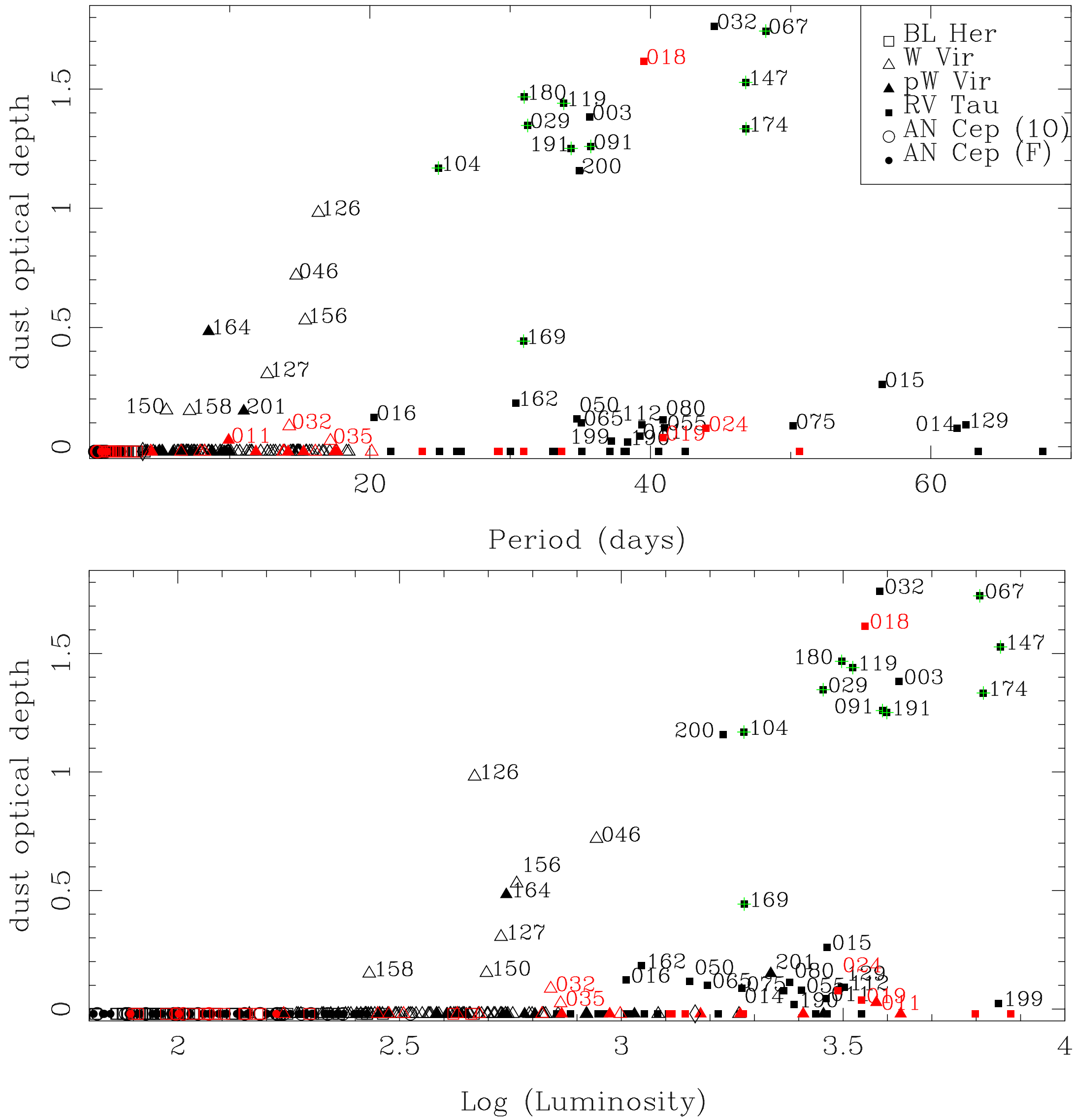

Excess below 1000 $L_{\odot}$!
Consistent with Kamath et al. (2016), starting from a sample of Post-AGB candidates.
"dusty post-red giant branch stars"
Binary pop. syn. models: have evolved off the RGB via binary interaction, and stored the dust in a circumbinary disc.

PL- PR relations

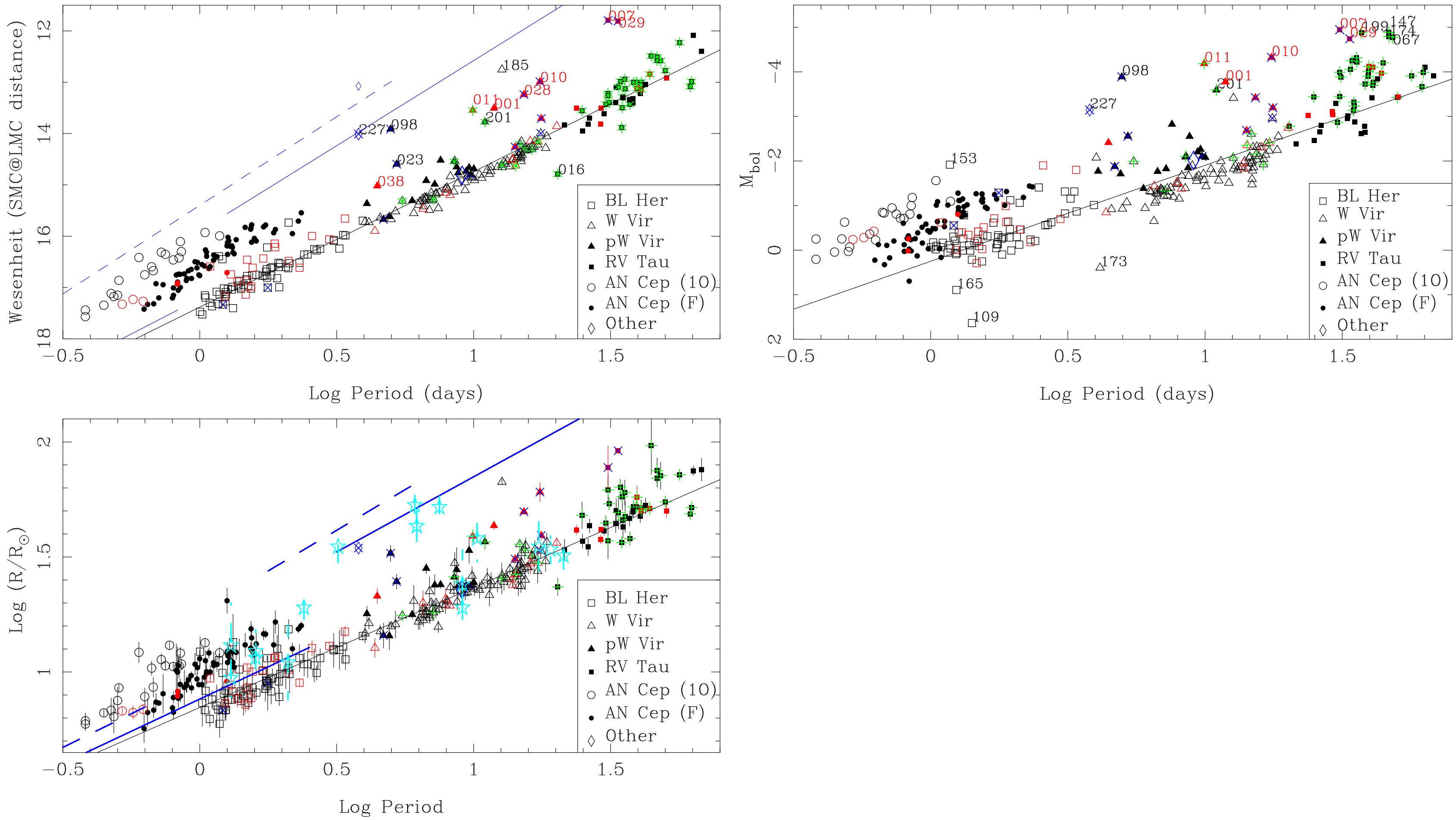

$PL-$, $PR-$ relations for AC, T2C
no difference between LMC and SMC
BLH, WVir, RVT can be combined
(with some restrictions)

Final remarks on T2C

- LITE $\Rightarrow \dot{P}$, Binary (OGLE-IV timeseries)
- Pulsation mass
- W Vir are unlikely to be related to TP on the AGB
- RVT more puzzling as a class ($\dot{P}$, mass)
- Galactic objects: Ph.D. by Joonas SAARIO (with Hans Van Winckel, KUL)
  - SED construction
  - GAIA parallax data
  - RV monitoring

Classical Cepheids: Pre-*Gaia*

- Compile metallicities ([Fe/H]) based on HR spectra for stars classified as CCs: 450

  Genovali et al (2014): 434 stars; compilation and put on uniform scale.
  Some other works: Ngeow, Luck & Lambert, Acharova et al., ...

- Types & Periods
  VSX (Variable Star indeX catalog) + other
  4 T2C, AHB, ROT

Pre-*Gaia*

- V, K photometry
  V: Mel'nik et al. (2015): 422 stars + other sources
  K:
  -intensity-mean: Monson & Pierre (2011), Laney & Stobie, Feast (SAAO), Welch, Barnes (CIT)
  -multiple single-epoch: scattered values
  -single-epoch 2MASS
- reddening $E(B-V)$
  Fernie et al. (1995): 400 stars + other sources (applying scaling)

Classical Cepheids and *Gaia*

- Main Catalog: position, PM, parallax, with errors. Statistical information on the fit

  `astrometric_chi2_al`, `astrometric_gof_al`

  GOF = $\sqrt{(9\nu/2)}\,[(\chi^2/\nu)^{\frac{1}{3}} + 2/(9\nu) - 1]$

  `astrometric_excess_noise`,
  `astrometric_excess_noise_sig`

  "measures how much the assumed observational noise in each observation must be (quadratically) increased in order to give $\chi^2 = \nu$ in the astrometric solution of the source"

- No binary motion was considered !

Classical Cepheids and *Gaia*

- "Degrees of Freedom" (DOF) bug (Appendix A in Lindegren et al.) All formal errors were scaled with an empirically determined factor.
  - Only approximate; errors could still be underestimated
  - All statistical parameters were not updated
- 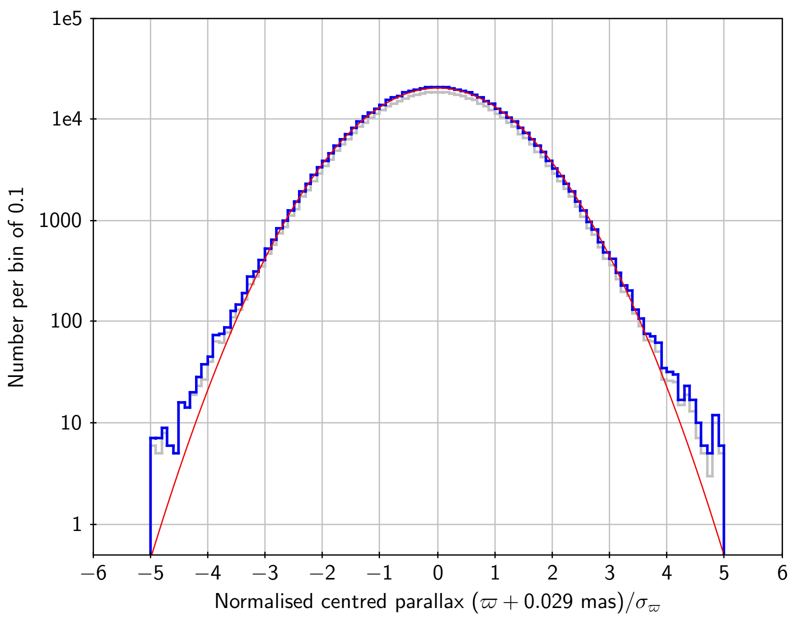

  parallax zero-point offset $\sim 500\ 000$ QSO (Lindegren et al.)

Classical Cepheids and *Gaia*

- The *Gaia* RR Lyrae and Cepheid Specific Objects Studies (SOS) module
  -The `type_best_classification` which can be DCEP, T2CEP, ACEP.
  -The `mode_best_classification` which can be FUNDAMENTAL, FIRST OVERTONE or MULTI.
  -The pulsation period with error.

Name	$\pi \pm \sigma_\pi$	GOF	ϵ_i	$\pi \pm \sigma_\pi$	GOF	$\pi \pm \sigma_\pi$	GOF	$\pi \pm \sigma_\pi$	$\pi \pm \sigma_\pi$
α UMi		271.0	7.5	7.56 ± 0.48	1.2	7.54 ± 0.11	1.1	7.72 ± 0.12	
Polaris B	7.292 ± 0.028	12.2	0.0						6.26 ± 0.24
δ Cep	-1.172 ± 0.468	182.2	2.4	3.32 ± 0.58	0.4	3.77 ± 0.16	-2.4	3.81 ± 0.20	3.66 ± 0.15
l Car	0.777 ± 0.257	171.1	1.7	2.16 ± 0.47	-0.5	2.09 ± 0.29	5.8	2.06 ± 0.27	2.01 ± 0.20
β Dor	3.112 ± 0.284	170.9	1.6	3.14 ± 0.59	-0.4	3.24 ± 0.36	13.8	3.64 ± 0.28	3.14 ± 0.16
ζ Gem	2.250 ± 0.301	90.1	1.2	2.79 ± 0.81	-0.3	2.37 ± 0.30	1.2	2.71 ± 0.17	2.78 ± 0.18
W Sgr	1.180 ± 0.412	88.2	1.4	1.57 ± 0.93	0.5	3.75 ± 1.12	10.4	2.59 ± 0.75	2.28 ± 0.20
X Sgr	3.431 ± 0.202	73.6	0.8	3.03 ± 0.94	0.6	3.31 ± 0.26	-0.6	3.39 ± 0.21	3.00 ± 0.18
Y Sgr	-0.470 ± 0.280	73.0	0.8	2.52 ± 0.93	-2.1	2.64 ± 0.45	-0.9	3.73 ± 0.32	2.13 ± 0.29
FF Aql	1.810 ± 0.107	65.8	0.5	1.32 ± 0.72	0.4	2.11 ± 0.33	0.7	2.05 ± 0.34	2.81 ± 0.18
RT Aur	1.419 ± 0.203	52.3	0.8	2.09 ± 0.89	-0.1	-1.10 ± 1.41	10.2	-0.23 ± 1.01	2.40 ± 0.19
T Vul	1.674 ± 0.089	44.5	0.3	1.95 ± 0.60	-0.2	2.71 ± 0.43	1.3	2.31 ± 0.29	1.90 ± 0.23
V1334 Cyg	1.151 ± 0.066	37.4	0.3	1.60 ± 2.20	-1.0	1.51 ± 0.37	7.9		1.39 ± 0.01
S Vul	0.305 ± 0.041	7.9	0.0						0.32 ± 0.04
RS Pup	0.584 ± 0.026	7.7	0.0	0.49 ± 0.68	-0.7	1.91 ± 0.65	0.7	1.44 ± 0.51	0.53 ± 0.02
XY Car	0.330 ± 0.027	7.5	0.0	-0.62 ± 0.95	-0.1	-1.02 ± 0.88	0.2	-0.75 ± 0.87	0.44 ± 0.05
SS CMa	0.201 ± 0.029	4.3	0.0	-0.37 ± 1.75	1.3	0.40 ± 1.78	1.8	0.35 ± 1.86	0.39 ± 0.03
VX Per	0.330 ± 0.031	3.8	0.0	1.08 ± 1.48	0.0	0.87 ± 1.52	1.1	1.10 ± 1.62	0.42 ± 0.07
WZ Sgr	0.513 ± 0.077	3.5	0.0	-0.75 ± 1.76	-0.4	3.50 ± 1.22	-0.1	2.46 ± 1.12	0.51 ± 0.04
SY Aur	0.313 ± 0.052	3.3	0.0	1.15 ± 1.70	0.3	-1.84 ± 1.72	1.3	-0.52 ± 1.44	0.43 ± 0.05
VY Car	0.512 ± 0.041	1.6	0.0	1.28 ± 1.76	2.8	0.36 ± 1.42	4.9	1.56 ± 0.91	0.59 ± 0.04
X Pup	0.302 ± 0.043	1.2	0.0	-0.05 ± 1.10	1.3	1.97 ± 1.26	-0.8	2.87 ± 0.92	0.28 ± 0.05

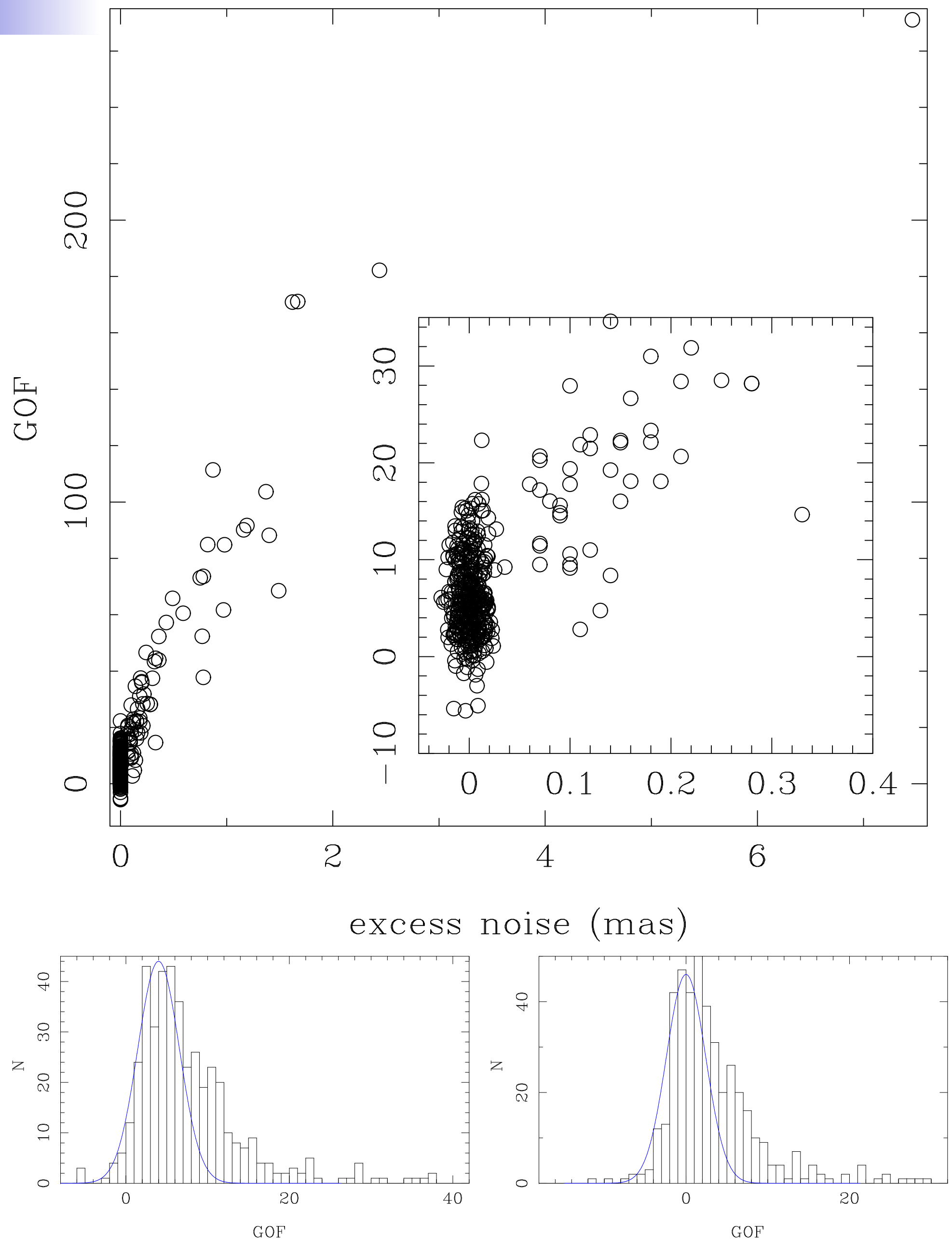

Goodness-of-Fit (Gaussian with mean 0, variance 1)

parallax zero-point offset

All 9 stars with a GOF < 8 have an accurate external parallax (σ_π comparable to that in GDR2).
The weighted mean difference (in the sense GDR2-external parallax) is -0.049 ± 0.018 mas.

-0.029 mas, QSO, Lindegren et al.

-0.046 ± 0.013 mas, 50 CCs (Riess et al.)
-0.053 ± 0.003 mas, RGB stars from *Kepler* and *APOGEE* data (Zinn et al. 2018)
(significant terms with G-mag and colour)
-0.056 ± 0.010 mas, RRL (Muraveva et al.)
-0.082 ± 0.033 mas, EBs (Stassun et al.)

Solving for the PL-relation

The fundamental equation between parallax, de-reddenned apparent and absolute magnitude is

$$\pi = 100 \cdot 10^{0.2\,(M-m)}$$

The absolute magnitude M is parameterised as

$$M = \alpha + \beta \, \log P + \gamma \, [\mathrm{Fe/H}]$$

Feast & Catchpole (1997) for Hipparcos data

-Symmetric errorbars
-No selection on parallax (error) [Lutz-Kelker bias]

Endless Solutions

- GOF $|\text{GOF}| < 8$
- For unreliable-*Gaia* parallax, take external parallax [or NOT]
- FU, fundamentalise FO FU
- Period range $2.7 < P(d) < 35$
- Parallax ZP offset
- V, K, WVK
- Systematic outliers
- (Simulations)

452 -6 non-DCEP -18 SO or DM -2 non-*Gaia*= 426
426 -GOF (-157, or 37%) -FO (-44, or 10%)
-Period range (-15) -outliers (-6) = 194-205

Bottom line

α, β, γ and parallax ZP offset are strongly correlated.

	α		β		Number	Remarks
1	-1.919	0.119	-2.386	0.138	194	V, GDR2
2	-1.875	0.118	-2.305	0.136	194	V, GDR2, ZPoff= -0.029
3	-1.848	0.119	-2.260	0.135	194	V, GDR2, ZPoff= -0.046
4	-2.912	0.058	-3.154	0.070	194	K, GDR2
5	-2.866	0.057	-3.071	0.068	194	K, GDR2, ZPoff= -0.029
6	-2.839	0.056	-3.028	0.067	194	K, GDR2, ZPoff= -0.046
7	-3.047	0.055	-3.252	0.066	194	WVK, GDR2
8	-2.999	0.053	-3.170	0.063	194	WVK, GDR2, ZPoff= -0.029
9	-2.972	0.052	-3.126	0.063	194	WVK, GDR2, ZPoff= -0.046

Slopes in LMC are significantly different

-2.810 (V); -3.260 (K), -3.325 (WVK)

Bottom line

	α		β		Number	Remarks	LMC DM
26	-1.589	0.030	-2.810	fixed	194	V, GDR2	18.761 $\pm$ 0.030
27	-1.480	0.030	-2.810	fixed	194	V, GDR2, ZPoff= -0.029	18.650
28	-1.418	0.030	-2.810	fixed	194	V, GDR2, ZPoff= -0.046	18.590
29	-1.321	0.030	-2.810	fixed	194	V, GDR2, ZPoff= -0.074	18.493
30	-1.233	0.030	-2.810	fixed	194	V, GDR2, ZPoff= -0.100	18.405
43	-2.827	0.014	-3.260	fixed	194	K, GDR2	18.880 $\pm$ 0.014
44	-2.717	0.014	-3.260	fixed	194	K, GDR2, ZPoff= -0.029	18.770
45	-2.655	0.014	-3.260	fixed	194	K, GDR2, ZPoff= -0.046	18.708
46	-2.469	0.013	-3.260	fixed	194	K, GDR2, ZPoff= -0.100	18.522
64	-2.988	0.013	-3.325	fixed	194	WVK, GDR2	18.858 $\pm$ 0.018
65	-2.878	0.013	-3.325	fixed	194	WVK, GDR2, ZPoff= -0.029	18.748
66	-2.816	0.013	-3.325	fixed	194	WVK, GDR2, ZPoff= -0.046	18.696
67	-2.784	0.012	-3.325	fixed	194	WVK, GDR2, ZPoff= -0.055	18.654
68	-2.714	0.012	-3.325	fixed	194	WVK, GDR2, ZPoff= -0.075	18.584
69	-2.630	0.012	-3.325	fixed	194	WVK, GDR2, ZPoff= -0.100	18.500

Summary

- Parallax ZP offset is a huge limitation
- Slopes MW may be different
- for Parallax ZP offset ~ -0.046, LMC DM ~ 18.7
- for Parallax ZP offset ~ -0.1, LMC DM ~ 18.5
  (trends also seen in the RRL)
- metallicity dependence is inconclusive
  including γ will lead to slightly lower LMC DM
  γ becomes $2 - 3\sigma$ effect, and larger than BW-analysis
  (Storm et al. 2011, Groenewegen 2013)

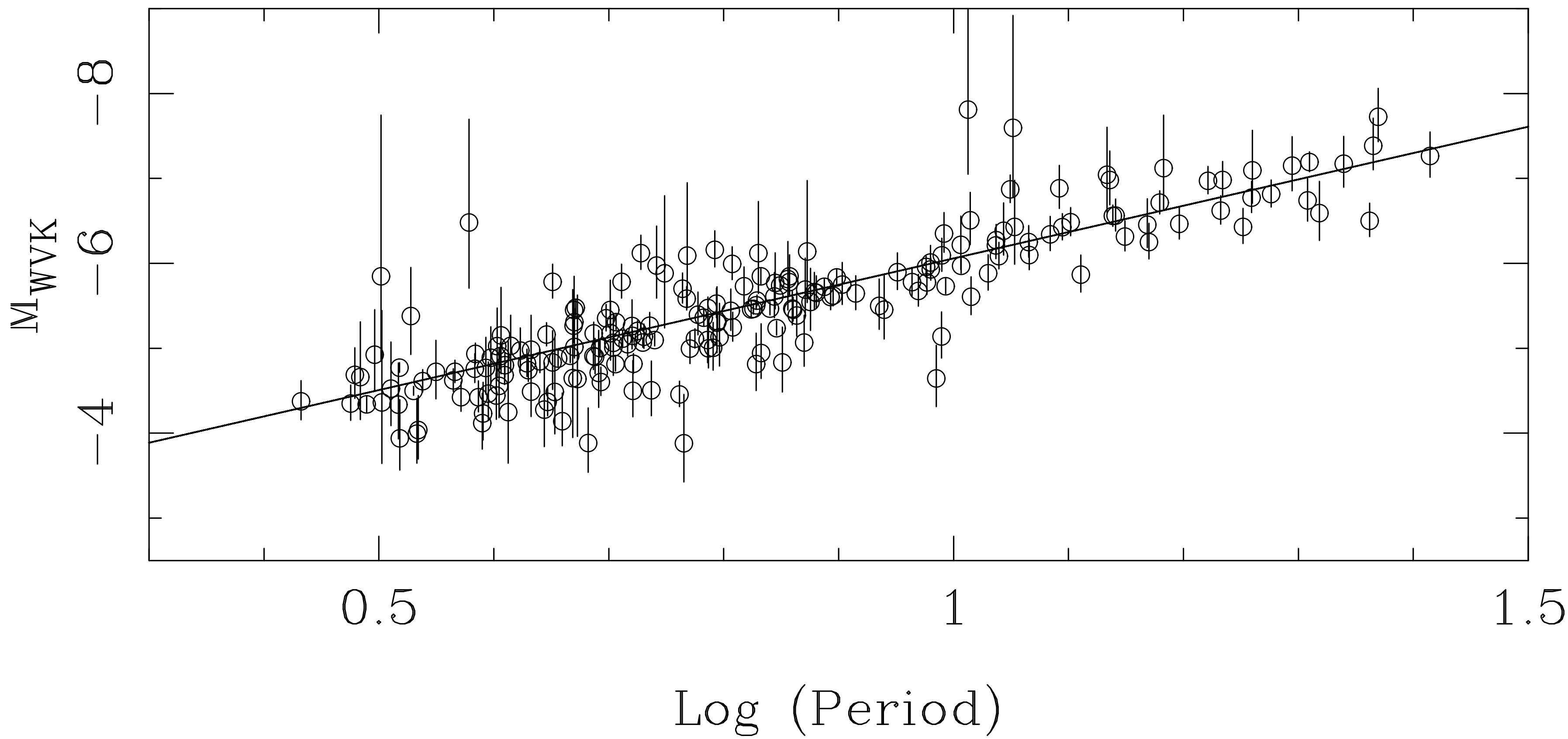

ZPoff$=-0.049$, $\gamma = 0$

$$M_{\rm WVK} = (-2.961 \pm 0.051) - (3.098 \pm 0.060) \log P$$

THE END